$$\ln(T_S/T_0) = \int_V^{V_0} \Gamma\, dV/V, \tag{17}$$

where

$$\Gamma \equiv \frac{V}{C_V}\left(\frac{\partial P}{\partial T}\right)_V, \tag{18}$$

is the Gruneisen ratio. The additional temperature increment at the same volume arising from shock compression is $T_D - T_S$, where

$$\ln T_D/T_S = \int_{S_0}^{S_D} dS/C_V. \tag{19}$$

Entropy, S_D, can be expressed as a series in powers of the volume compression, $\eta = (1 - V/V_0)$:

$$S_D - S_0 = \frac{V_0^3}{12T_0}\eta^3\left(\frac{\partial^2 P}{\partial V^2}\right)_0 + \cdots, \tag{20}$$

where the second derivative is evaluated for the initial state on the isentrope or the R–H curve. If C_V and Γ/V are assumed constant, Eqs. (17), (19), and (20) can be combined to give

$$\ln T_D/T_0 = \Gamma_0\eta\left[1 + \frac{V_0^2\eta^2}{12\alpha T_0 K_0}\left(\frac{\partial^2 P}{\partial V^2}\right)_0 + \cdots\right], \tag{21}$$

where α is the thermal expansion coefficient, K_0 is the isothermal bulk modulus at (V_0, T_0) and Γ_0 has been evaluated by Eq. (18). For an R–H curve given by Eq. (16), Eq. (21) becomes

$$\ln T_D/T_0 = \Gamma_0\eta\left[1 + \frac{1+s}{6T_0\alpha}\eta^2 + \cdots\right]. \tag{22}$$

Coefficients of η^2 range from 10 to 100 for a variety of solids, so the temperature increment from irreversible shock heating is negligible for volume compressions of a few percent.

The problem represented by Figs. 2 and 3 is not realized in practice. Half-spaces do not exist, and uniform pressure cannot be instantly applied over a surface. Limitations imposed by real conditions are discussed in Sec. III.

C. Shock-wave stability

In general the R–H curve is not so simple as that shown in Fig. 3. A more common type for a solid has a cusp where elastic failure occurs, and a solid which fails elastically and also transforms to a new phase under pressure has two cusps, as shown in Fig. 4. In such a case the simple wave structure of Fig. 2(b) no longer applies. Instead the wave may consist of one, two, or three shock fronts, each one separating uniform states, depending on location of cusps and the magnitude of P_1, Fig. 5. In that case the jump conditions, Eqs. (9)–(11), are written for the ith shock:

$$p_x^i - p_x^{i-1} = (U_s^i - U_p^{i-1})(U_p^i - U_p^{i-1})/V_{i-1}, \tag{23}$$

$$1 - V_i/V_{i-1} = (U_p^i - U_p^{i-1})/(U_s^i - U_p^{i-1}), \tag{24}$$

$$E_i - E_{i-1} = (p_x^i + p_x^{i-1})(V_{i-1} - V_i)/2, \tag{25}$$

where p_x^i, V_i, U_p^i, and E_i are values of state variables behind the shock; p_x^{i-1}, V_{i-1}, U_p^{i-1}, and E_{i-1} are values ahead of it; and U_s^i is its velocity of propagation.

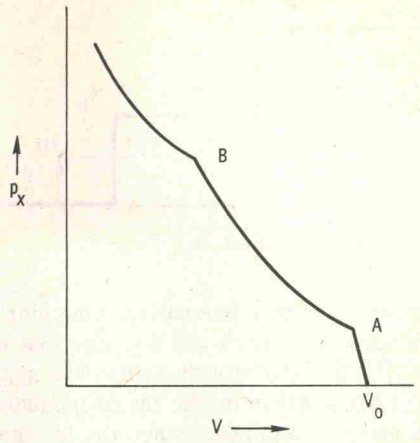

FIG. 4. R–H curve centered at (P_0, V_0) for a solid which fails elastically at A and transforms to a new phase starting at B.

Division of the shock wave into multiple waves hinges on questions of stability. Whether or not a given shock wave configuration is stable can be simply expressed by determining whether following shock waves will overtake those in front (Rice *et al.*, 1958). For example, in Fig. 6 are represented two shock waves in sequence. The leading shock S_1 is traveling with speed $U_s^{(1)}$ relative to the material ahead of it, which is at rest. Material between S_1 and S_2 is compressed to specific volume V_1 and accelerated to particle velocity $U_p^{(1)}$. With respect to this material the first shock speed is $U_s^{(1)} - U_p^{(1)}$. With respect to this same material the second shock has speed $U_s^{(2)} - U_p^{(1)}$. If $U_s^{(2)} - U_p^{(1)} < U_s^{(1)} - U_p^{(1)}$, the second shock falls continually farther behind the first shock, and the two-shock system is stable. If the inequality is reversed, the second shock overtakes the first, forming a single stable shock.

From Eqs. (9) and (10) the equation for shock propagation speed is obtained

$$(U_s^i - U_p^{i-1})^2 = V_{i-1}^2(p_x^i - p_x^{i-1})/(V_{i-1} - V_i) \tag{26}$$

also

$$U_s^i - U_p^i = (V_i/V_{i-1})(U_s^i - U_p^{i-1}). \tag{27}$$

Applying these equations to the two shocks of Fig. 6, we see that the double shock is stable if

$$\frac{p_x^{(2)} - p_x^{(1)}}{V_1 - V_2} < \frac{p_x^{(1)} - P_0}{V_0 - V_1}. \tag{28}$$

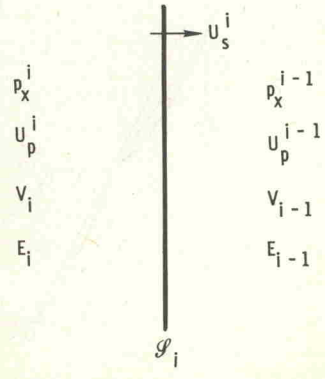

FIG. 5. Parameters of a shock preceded by moving material.

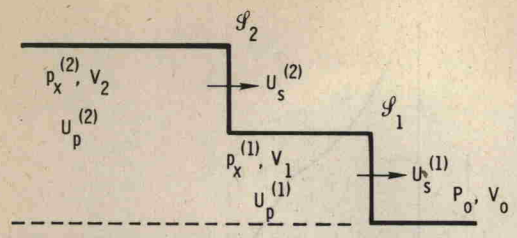

FIG. 6. Double shock configuration.

To see the meaning of this inequality, consider the (p_x, V) curve shown in Fig. 7 and suppose that the final shock state $(p_x^{(2)}, V_2)$ of Fig. 6 is at B. The negative slope of chord AB is given by the lhs of Inequality (28); that of OA is given by the rhs. Since OA is steeper than AB, Inequality (28) is satisfied and a double shock to B, with break at A, is stable. Chords like OA and AB of Fig. 7 which connect initial and final states are sometimes called "Rayleigh lines." If the driving pressure $p_x^{(2)}$ lies between O and A or above C, a single shock is stable. If it lies between A and C, a double shock is stable.

The shock stability problem can be couched more fundamentally in terms of the curvature of isentropes for a fluid medium (Bethe, 1942; Duvall, 1962). If

$$(\partial^2 P/\partial V^2)_s < 0$$

in some region, then there exist initial and final states for which a single shock wave is not stable. The general theory of stability is complicated (Fowles, 1976), but Inequality (28) is an adequate rule for practical experimental purposes.

D. Transformation thermodynamics

Gibbs (1925) was among the earliest thermodynamicists to point out the utility of geometric representations in thermodynamics. Such representations are particularly appropriate for discussion of shock phenomena since many important qualitative aspects of shock-wave representation are related to topological features of equation of state surfaces, without reference to particular analytical forms or numerical values. Some equilibrium relations pertaining to shock-induced phase transformations are described in this section.

Consider only a material that retains its chemical identity but can exist in two distinguishable physical forms, e.g., red and black phosphorus. Consider further that stress is limited to hydrostatic pressure. Then there exists a Gibbs function for each phase

$$G_i(P, T) = E_i - TS_i + PV_i, \quad i = 1, 2, \tag{29}$$

where S_i is specific entropy for phase i. The high-density phase will be referred to as "phase 2" throughout this paper.

Equations (29) represent two surfaces in a three-dimensional space with coordinates G, P, T, where $G = G_1$ for phase 1 and G_2 for phase 2. Transition between phases occurs where the two surfaces are in contact. If they intersect, the transition is first order and the Clausius–Clapeyron equation is the differential equation of the curve of intersection projected on the $P-T$ plane

$$dP/dT = (S_2 - S_1)/(V_2 - V_1) \equiv \Delta S/\Delta V. \tag{30}$$

The discontinuities in V and S arise from their identity as derivatives of G

$$V = \partial G/\partial P, \quad S = -\partial G/\partial T,$$

where the underlying surface represents the equilibrium state. This is illustrated in Fig. 8, where $G_1(P, T_0)$ and $G_2(P, T_0)$ are shown. $G(P, T_0)$ is the curve ABC.

If the two surfaces do not intersect, but are tangent along a curve, the transition is second order and second derivatives of G are discontinuous. Higher-order contacts define higher-order transitions, but these are hard to detect experimentally (Temperley, 1956). Our primary concern is with first-order transitions, though second-order transitions will be discussed briefly in Sec. V.

Discontinuities in V and S define a "mixed phase" region in $P-V-T$ space where phases 1 and 2 coexist. The mixed phase region is a cylindrical surface with generatrix normal to the $P-T$ plane. The phase diagram in the $P-T$ plane is the projection of this cylinder onto the $P-T$ plane. On the cylindrical surface Eq. (30) applies. If phase 2 is the high-pressure phase, $\Delta V < 0$ and ΔS may be either negative or positive. In the former case, $dP/dT > 0$; in the latter, $dP/dT < 0$. These two equilibrium cases are illustrated in Figs. 9 and 11, respectively. It can be seen from these figures that both cases

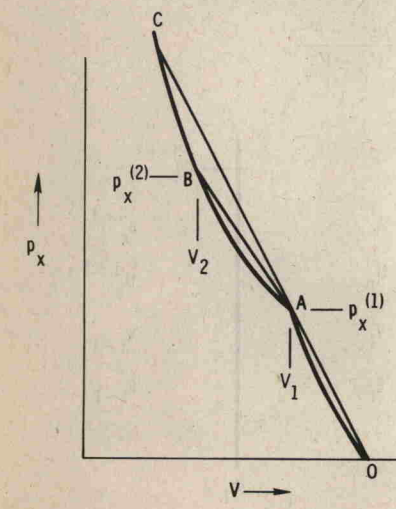

FIG. 7. Stability considerations for a double shock.

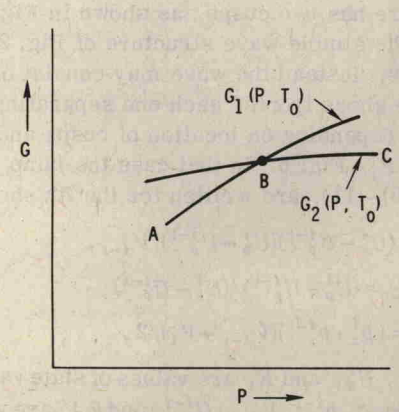

FIG. 8. Gibbs functions for a first-order transition.